J. Plasma Phys. (2025), *vol.* 91, E52 © The Author(s), 2025. Published by Cambridge University Press.
This is an Open Access article, distributed under the terms of the Creative Commons Attribution licence (https://creativecommons.org/licenses/by/4.0/), which permits unrestricted re-use, distribution and reproduction, provided the original article is properly cited. doi:10.1017/S0022377825000236

Transmission and reflection of the dust acoustic wave at an interface in an inhomogeneous dusty plasma

Zhong-Zheng Li[1] and **Wen-Shan Duan**[1,2]

[1]School of Energy and Power Engineering, Gansu Minzu Normal University, Hezuo 747000, PR China
[2]College of Physics and Electronic Engineering, Northwest Normal University, Lanzhou 730070, PR China

Corresponding author: Wen-Shan Duan, duanws@nwnu.edu.cn

(Received 7 April 2024; revision received 23 February 2025; accepted 24 February 2025)

Dusty plasmas typically contain various species of dust particles, though most studies have focused on homogeneous systems. This paper investigates the propagation of dust acoustic waves in an inhomogeneous dusty plasma with an interface, analysing how plasma inhomogeneity influences wave behaviour. Using scattering and reductive perturbation methods, we show that both transmitted and reflected waves depend strongly on the mass ratio between regions. Dust acoustic waves cannot propagate through a dust lattice when the wavelength is smaller than the lattice constant. At a discontinuous interface, at least one transmitted solitary wave is generated, with its amplitude determined by the mass ratio, while at most one reflected solitary wave can exist. These results underscore the critical role of the mass ratio in wave propagation and suggest a method for estimating dust particle masses and properties by analysing the incident, transmitted and reflected waves.

Keywords: Solitary waves, Plasmas

1. Introduction

A dusty plasma consists of charged micrometer-sized dust particles, free electrons, free ions and neutrals (Rao, Shukla & Yu 1990; Mendis & Rosenberg 1994; Barkan *et al.* 1995, 1996; I *et al.* 1996; Murillo 2000; Kalman *et al.* 2004; Morfill & Ivlev 2009; Ghosh *et al.* 2011; Shukla & Eliasson 2012; Melzer *et al.* 2013; Thomas *et al.* 2016). The interaction potential between two dust particles is typically described by the Yukawa potential $\phi(r) = (q/4\pi\varepsilon_0 a)\exp(a/\lambda_D)$, where a is the distance between the particles, q is the dust particle charge, ε_0 is the vacuum permittivity and λ_D is the Debye length of the dusty plasma.

For simplicity and generality, two parameters are commonly introduced in a dusty plasma (Feng *et al.* 2016; Li & Duan 2021). One is the coupling parameter, $\Gamma =$

Downloaded from https://www.cambridge.org/core. IP address: 18.189.178.124, on 06 Apr 2025 at 16:28:04, subject to the Cambridge Core terms of use, available at https://www.cambridge.org/core/terms. https://doi.org/10.1017/S0022377825000236

$(Q^2/4\pi\varepsilon_0 a)(1/k_B T_d)$, and the other is the screening parameter, $\kappa = (a/\lambda_D)$, where k_B is the Boltzmann constant and T_d is the temperature of the dust particle fluid. A dusty plasma can be in the gas, the liquid or the solid state, which depends on the values of both parameters Γ and κ. For example, if $\Gamma \geqslant 10^2$, a dusty plasma may form a dusty plasma crystal.

There is a substantial body of research on dusty plasma (Thomas *et al.* 1994; Homann *et al.* 1997; Melzer *et al.* 2000; Nunomura *et al.* 2002; Liu, Avinash & Goree 2003; Nosenko, Goree & Piel 2006; Koukouloyannis & Kourakis 2009; Heinrich, Kim & Merlino 2009; Feng, Goree & Liu 2010; Oxtoby *et al.* 2013; Marciante & Murillo 2017; Lin, Murillo & Feng 2019; Houwe *et al.* 2022). However, most of the previous work has focused on dusty plasmas composed of identical dust particles. Nevertheless, experimental results show that dusty plasmas in both space and laboratory environments contain a variety of dust particles (Horanyi & Goertz 1990; Chow, Mendis & Rosenberg 1993; Meuris, Verheest & Lakhina 1997; Duan 2001). It has been found that the dust size distribution plays a crucial role in the characteristics of a dusty plasma (Duan & Parkes 2003; Duan & Shi 2003; Duan *et al.* 2007).

Recently, dusty plasmas containing two or more different microparticles with different sizes have been studied (Smith *et al.* 2008; Hartmann *et al.* 2009; Ivlev *et al.* 2009; Jiang *et al.* 2011; Wieben, Schablinski & Block 2017). A series of experiments on binary complex plasmas over a broad range of parameters has also been conducted (Du *et al.* 2012; Killer *et al.* 2016).

The wave phenomenon in plasmas has attracted considerable attention (Sergeev & Grach 2014; He *et al.* 2016; Xu & Song 2019). The waves in a binary dusty plasma have also been studied (Yang *et al.* 2017; Sun *et al.* 2018). The slow dynamics in dusty plasmas with two different dust sizes were experimentally studied by Du *et al.* (2019). Moreover, the reflection and transmission of a solitary wave across an interface in a binary complex plasma have been examined numerically, experimentally and analytically (Hong *et al.* 2021).

A dusty plasma usually contains different species of dust particles both in space plasma and in laboratory experiments. However, most previous studies on the dusty plasma focussed on the dust plasma in which all the dust particles are assumed to be the same. How a wave propagates in an inhomogeneous dusty plasma composed of different species of the dust particles remains an interesting question with many unresolved problems. Recently, experimental investigations on a dust acoustic wave propagating to an interface were reported (Du *et al.* 2019; Kumar *et al.* 2021). Subsequently, studies examined how an incident pulse wave is transmitted and reflected by several impurity dust particles (Wei *et al.* 2023). Following the previous works, the present paper investigates how both the linear wave and the nonlinear wave are reflected and transmitted by an interface, as reported in experiments (Du *et al.* 2019). It has been found that both the transmitted and reflected waves not only depend on the incident wave, but also are strongly influenced by the mass ratio between the two regions. It appears that the dust acoustic wave cannot propagate through the dust lattice if the wavelength is smaller than the dust lattice constant. Additionally, it has been observed that at least one transmitted solitary wave is generated when an incident solitary wave reaches a discontinuous interface. However, there is at most one reflected solitary wave. Based on these results, an experiment can be designed to estimate the mass of the dust particles and the distribution of different dust species by sending an incident wave through the inhomogeneous region and measuring the transmitted and reflected wave information.

Downloaded from https://www.cambridge.org/core. IP address: 18.189.178.124, on 06 Apr 2025 at 16:28:04, subject to the Cambridge Core terms of use, available at https://www.cambridge.org/core/terms. https://doi.org/10.1017/S0022377825000236

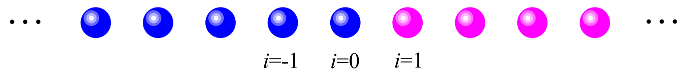

FIGURE 1. Schematic of a one-dimensional dust particle chain, in which the blue spheres are one kind of dust particles, while the magenta spheres are another kind of dust particles.

This paper is organised as follows. Section 2 establishes the model used in the present study. Section 3 gives linear wave propagation and its dispersion relation. Section 4 discusses the continuity condition when a wave propagates across a discontinuous interface. Section 5 examines the transmission and reflection of an incident solitary wave by the discontinuous interface. Section 6 provides the conclusion for the present paper.

2. Model

It has been recently reported that a binary complex plasma was formed by injecting two types of particles under microgravity conditions in the PK-3 Plus laboratory onboard the International Space Station (ISS). One type consists of melamine formaldehyde particles with a diameter of 2.55 μm and a mass of $m = 1.34 \times 10^{-14}$ kg, while the other consists of SiO_2 particles with a diameter of 1.55 μm and a mass of $m = 3.6 \times 10^{-15}$ kg. Due to differences in particle properties, phase separation occurred, leading to the formation of an interface between the two types of particles (Du *et al.* 2019; Hong *et al.* 2021). In this study, we consider a strongly coupled regime where the coupling strength satisfies $\Gamma > 100$, ensuring that the dusty plasma is in a solid-state condition. Based on this, we now consider an inhomogeneous dust particle chain consisting of an homogeneous chain of N identical dust particles from $i = -N + 1$ to $i = 0$, and another homogeneous chain of N identical dust particles from $i = 1$ to $i = N$. However, the dust particles differ in the regions $i = -N + 1$ to $i = 0$ $(x < 0)$ and $i = 1$ to $i = N$ $(x > 0)$, as shown in figure 1.

We now aim to understand the following phenomena. Suppose that a wave propagates in the region $i < 0$ $(x < 0)$ and moves towards the region $i > 0$ $(x > 0)$. When it reaches the discontinuity at $x = 0$, it will evolve into a transmitted wave in the region $x > 0$ and a reflected wave in the region $x < 0$. In this case, the region $x > 0$ will contain only the transmitted wave, while the region $x < 0$ will contain both the incident and reflected wave.

When there are perturbations in a dust particle chain, we assume that the position of dust particle i is given by $x_i = ia_0 + \xi_i$, where ξ_i is the displacement of dust particle i from its equilibrium position ia_0 and a_0 is the lattice constant representing the distance between neighbouring dust particles in the equilibrium state. For simplicity and convenience, we express ξ_i as ξ_i^Z, where Z can be I, R or T for the incident, reflected or transmitted wave, respectively.

For an arbitrary dust particle i, the equation of motion is given by $m_d\ddot{\boldsymbol{\xi}}_i = -q\nabla \sum_{j\neq i} \phi_{ij}$, where m_d and q are the mass and charge of the dust particle, ϕ_{ij} is the Yukawa interaction potential between dust particles of i and j, $\phi_{ij} = q/4\pi\varepsilon_0 x_{ij} e^{-\frac{x_{ij}}{\lambda_D}}$, where $x_{ij} = |x_i - x_j|$ is the distance between dust particles i and j, λ_D is the Debye length, and ε_0 is the permittivity of vacuum.

Due to the shielding effect, we consider only the interaction forces between nearest-neighbouring dust particles. We also use two approximations. First, the small

Downloaded from https://www.cambridge.org/core. IP address: 18.189.178.124, on 06 Apr 2025 at 16:28:04, subject to the Cambridge Core terms of use, available at https://www.cambridge.org/core/terms. https://doi.org/10.1017/S0022377825000236

amplitude approximation $a_0 \gg \xi_i - \xi_{i-1}$. The small amplitude approximation means that the displacement difference between the nearest neighbours of the dust particles $(\xi_i - \xi_{i-1})$ is much less than the lattice constant (a_0). Second, the long wavelength approximation $a_0 \ll \lambda$, where λ is the wavelength of the perturbations. In other words, the long wave approximation means that the wavelength is much larger than the lattice constant. By using the small amplitude approximation and Taylor expansions, we have $m_d(\partial^2\xi_i/\partial t^2) = k_1(\xi_{i+1} + \xi_{i-1} - 2\xi_i) + k_2[(\xi_{i+1} - \xi_i)^2 - (\xi_i - \xi_{i-1})^2] + O[(\xi_{i+1} - \xi_i)^3 - (\xi_i - \xi_{i-1})^3]$, where $k_1 = (q^2/4\pi\varepsilon_0 a_0^3)e^{-\kappa}[2 + 2\kappa + \kappa^2]$, $k_2 = -(q^2/8\pi\varepsilon_0 a_0^4)e^{-\kappa}[6 + 6\kappa + 3\kappa^2 + \kappa^3]$. By using the long wavelength approximation and the continuum approximation $\xi_i(t) = \xi(x, t)$, we have $\xi_{i\pm1,t} = \xi(x, t) \pm (\partial\xi/\partial x)a_0 + (a_0^2/2)(\partial^2\xi/\partial x^2) \pm (a_0^3/6)(\partial^3\xi/\partial x^3) + (a_0^4/24)(\partial^4\xi/\partial x^4) + \cdots$. Since all the physical quantities are functions of time t and the spatial coordinate i, where i is a discrete integer variable, for simplicity and convenience, we can treat i as x, where x is a continuous variable. This is known as the continuum approximation. Furthermore, due to the small amplitude approximation, Taylor expansion can be applied. Consequently, we obtain the equation of motion for the dust particle as follows (Wei *et al.* 2023):

$$\frac{\partial^2\xi}{\partial t^2} = B_1\left(\frac{\partial^2\xi}{\partial x^2} + \frac{a_0^2}{12}\frac{\partial^4\xi}{\partial x^4}\right) + B_2\frac{\partial\xi}{\partial x}\frac{\partial^2\xi}{\partial x^2}, \tag{2.1}$$

where $B_1 = k_1a_0^2/m_d$ and $B_2 = 2k_2a_0^3/m_d$.

3. Linear wave and dispersion relation

For a small amplitude wave (i.e. a linear wave), (2.1) reduces to a linear equation as

$$\frac{\partial^2\xi}{\partial t^2} = B_1\left(\frac{\partial^2\xi}{\partial x^2} + \frac{a_0^2}{12}\frac{\partial^4\xi}{\partial x^4}\right). \tag{3.1}$$

For a linear wave, we assume that $\xi = \xi_0 e^{i(kx-\omega t)}$. The dispersion relation from (3.1) is given by $\omega^2 = B_1k^2(1 - (a_0^2/12)k^2)$, or $\omega = \pm\sqrt{B_1}k\sqrt{(1 - (a_0^2/12)k^2)}$. The phase speed is $v_p = \omega/k = \pm\sqrt{B_1}\sqrt{(1 - (a_0^2/12)k^2)}$. It appears that there are no real values for ω if $a_0^2k^2 > 12$, which indicates that the waves cannot propagate in the dust chain if the wavelength is small enough. The critical wavenumber is $k_c = 2\sqrt{3}/a_0$. Waves exist if $k < k_c$, but do not exist if $k > k_c$.

The natural frequency in the dust lattice chain is $\omega_0 = \sqrt{k_1/m_d}$. For the long wavelength approximation, i.e. $a_0k << 1$, we have $v_p = \sqrt{B_1} = \omega_0 a_0$.

4. Continuity equation

Suppose there is an incident wave propagating in the positive x direction in the region $x < 0$. When it reaches the discontinuity point $x = 0$, it will be both reflected and transmitted at this point. We now aim to construct both the reflected wave and transmitted waves from the incident wave. To do this, we use the continuity condition at $x = 0$.

The momentum of the dust particles and the force acting on them at the interface $x = 0$ should be continuous. Neglecting higher-order terms and applying the continuity conditions at the interface $x = 0$, we have

Downloaded from https://www.cambridge.org/core. IP address: 18.189.178.124, on 06 Apr 2025 at 16:28:04, subject to the Cambridge Core terms of use, available at https://www.cambridge.org/core/terms. https://doi.org/10.1017/S0022377825000236

$$\frac{m_d^-}{a_0^{-3}}\frac{\partial \xi^I}{\partial t}\mid_{x=0} + \frac{m_d^-}{a_0^{-3}}\frac{\partial \xi^R}{\partial t}\mid_{x=0} = \frac{m_d^+}{a_0^{+3}}\frac{\partial \xi^T}{\partial t}\mid_{x=0}, \tag{4.1}$$

$$k_1^-\xi^I\mid_{x=0} + k_1^-\xi^R\mid_{x=0} = k_1^+\xi^T\mid_{x=0}, \tag{4.2}$$

where m_d^- and m_d^+ are the mass of the dust particles in the regions $x<0$ and $x>0$, respectively. Here, k_1^- and k_1^+ correspond to the parameters of k_1 in the regions $x<0$ and $x>0$, respectively. For the three-dimensional case, $n_d^- = 1/a_0^{-3}$ and $n_d^+ = 1/a_0^{+3}$.

4.1. *Reflection and transmission by linear incident wave*

We first study the transmission and reflection of an incident linear wave. For convenience and generality, we assume that $\xi^I = \xi_0^I e^{k_I x-\omega t}$, $\xi^R = \xi_0^R e^{k_R x-\omega t}$ and $\xi^T = \xi_0^T e^{k_T x-\omega t}$, where ξ_0^I, ξ_0^R and ξ_0^T are the wave amplitude of the incident wave, reflected and transmitted waves, respectively. Here, ω is the wave frequency, and k_I, k_R and k_T are the wavenumbers for the incident, reflected and transmitted wave, respectively. We have $k_I = k_R = (\omega/\sqrt{B_1^-})$, $k_T = (\omega/\sqrt{B_1^+})$, $B_1^- = (k_1^-(a_0^-)^2)/rm_d^-$ and $B_1^+ = (k_1^+(a_0^+)^2)/m_d^+$. We derive these results from (4.1) and (4.2),

$$\xi_0^T = \frac{2}{\chi_m + \chi_k}\xi_0^I, \tag{4.3}$$

$$\xi_0^R = \frac{\chi_k - \chi_m}{\chi_m + \chi_k}\xi_0^I, \tag{4.4}$$

where $\chi_m = m_d^+/m_d^-(a_)^-/a_0^+)^3$, $\chi_k = k_1^+/k_1^-$. The amplitude ratios of both the transmitted wave to the incident wave and the reflected wave to the incident wave are

$$\frac{\xi_0^T}{\xi_0^I} = \frac{2}{\frac{m_d^+}{m_d^-}(\frac{a_)^-}{a_0^+})^3 + \frac{q^+}{q^-}(\frac{a_0^-}{a_0^+})^3\frac{2+2\kappa^+ + (\kappa^+)^2}{2+2\kappa^- + (\kappa^-)^2}e^{(\kappa^- - \kappa^+)}}, \tag{4.5}$$

$$\frac{\xi_0^R}{\xi_0^I} = \frac{1 - \frac{m_d^+}{m_d^-}\frac{q^-}{q^+}\frac{2+2\kappa^- + (\kappa^-)^2}{2+2\kappa^+ + (\kappa^+)^2}e^{(\kappa^+ - \kappa^-)}}{1 + \frac{m_d^+}{m_d^-}\frac{q^-}{q^+}\frac{2+2\kappa^- + (\kappa^-)^2}{2+2\kappa^+ + (\kappa^+)^2}e^{(\kappa^+ - \kappa^-)}}, \tag{4.6}$$

where $\kappa^+ = a_0^+/\lambda_D^+$, $\kappa^- = a_0^-/\lambda_D^-$ are the screening parameters in the region of $x>0$ and $x<0$, respectively. Here, $\lambda_D^+ = [(n_e^+e^2/\epsilon_0 k_B T_e^+) + (Z_i^2 n_i^+ e^2/\epsilon_0 k_B T_i^+)]^{-1/2}$, $\lambda_D^- = [(n_e^- e^2/\epsilon_0 k_B T_e^-) + (Z_i^2 n_i^- e^2/\epsilon_0 k_B T_i^-)]^{-1/2}$ are the Debye length in the regions of $x>0$ and $x<0$, respectively, n_e^+, T_e^+, n_i^+ and T_i^+ are the number density, the temperature of the electrons, the number density and the temperature of the ions in the region $x>0$, respectively, n_e^-, T_e^-, n_i^- and T_i^- are the number density, the temperature of the electrons, the number density and the temperature of the ions in the region $x<0$, respectively, and q^+ and q^- are the electric charge of a dust particle in the region $x>0$ and region $x<0$, respectively. The electric charge neutrality in two regions yields $n_e^+e - Z_i^+n_i^+e + (q^+/(a_0^+)^3) = 0$, $n_e^-e - Z_i^-n_i^-e + (q^-/(a_0^-)^3) = 0$, where we used the equation of $a_0 = n_d^{-1/3}$ for a three-dimensional dusty plasma (Hong *et al.* 2021).

Downloaded from https://www.cambridge.org/core. IP address: 18.189.178.124, on 06 Apr 2025 at 16:28:04, subject to the Cambridge Core terms of use, available at https://www.cambridge.org/core/terms. https://doi.org/10.1017/S0022377825000236

At equilibrium, the variables of a_0^+ and a_0^- should be interdependent because the force in the dust particle chain must be a constant. Consequently, the following relationship holds: $k_1^+ a_0^+ + k_2^+ (a_0^+)^2 = k_1^- a_0^- + k_2^- (a_0^-)^2$. Thus, we have

$$\frac{a_0^+}{a_0^-} = \sqrt{\frac{q_d^-}{q_d^+} \frac{2 + 2\kappa^- + (\kappa^-)^2}{2 + 2\kappa^+ + (\kappa^+)^2} e^{(\kappa^+ - \kappa^-)}}. \tag{4.7}$$

Now consider the limiting case where $a_0 << \lambda_D$. In this case, (4.7) simplifies to

$$\frac{a_0^+}{a_0^-} = \sqrt{\frac{q_d^-}{q_d^+}}. \tag{4.8}$$

Equations (4.5) and (4.6) become

$$\frac{\xi_0^T}{\xi_0^I} = \frac{2}{\frac{m_d^+}{m_d^-}(\frac{a_)^-}{a_0^+})^3 + (\frac{a_0^-}{a_0^+})^5}, \tag{4.9}$$

$$\frac{\xi_0^R}{\xi_0^I} = \frac{1 - \frac{m_d^+}{m_d^-}(\frac{a_0^+}{a_0^-})^2}{1 + \frac{m_d^+}{m_d^-}(\frac{a_0^+}{a_0^-})^2}. \tag{4.10}$$

Furthermore, if all the dust particles are made of the same material and each dust particle is a spherical grain, then $m_d = 4/3\pi r_d^3$, where r_d is the dust particle radius. Additionally, $q \sim r_d^\gamma$, with $1 < \gamma < 2$ (Hong *et al.* 2021). Therefore, we have $a_0^+/a_0^- = (m_d^+/m_d^-)^{-\frac{\gamma}{6}}$, $q^+/q^- = (m_d^+/m_d^-)^{\frac{\gamma}{3}}$.

Equations (4.9) and (4.10) become

$$\frac{\xi_0^T}{\xi_0^I} = \frac{2}{(\frac{m_d^+}{m_d^-})^{\frac{4\gamma}{3}} + (\frac{m_d^+}{m_d^-})^{\frac{5\gamma}{6}}}, \tag{4.11}$$

$$\frac{\xi_0^R}{\xi_0^I} = \frac{1 - (\frac{m_d^+}{m_d^-})^{1-\frac{\gamma}{3}}}{1 + (\frac{m_d^+}{m_d^-})^{1-\frac{\gamma}{3}}}. \tag{4.12}$$

Figure 2 shows the dependence of the amplitude ratio (ξ_0^T/ξ_0^I) of the transmitted wave to the incident wave on the mass ratio (m_d^+/m_d^-), where the parameter $\gamma = 1, 1.5, 2$ (Hong *et al.* 2021). It shows that the amplitude ratio of the transmitted wave to the incident wave decreases as the dust particle mass ratio of that in the region $x > 0$ to that in the region $x < 0$ increases. In other words, the transmitted wave amplitude decreases for a given incident wave if the incident wave propagates from the smaller dust particle mass region to that of the larger dust particle mass region, while the transmitted wave amplitude increases if the incident wave propagates from the larger dust particle mass region to that of the smaller dust particle mass region. It is also shown that the amplitude ratio of the transmitted wave to the incident wave increases as the parameter γ increases in the region $m_d^+/m_d^- < 1$, while it decreases as the parameter γ increases in the region $m_d^+/m_d^- > 1$.

Downloaded from https://www.cambridge.org/core. IP address: 18.189.178.124, on 06 Apr 2025 at 16:28:04, subject to the Cambridge Core terms of use, available at https://www.cambridge.org/core/terms. https://doi.org/10.1017/S0022377825000236

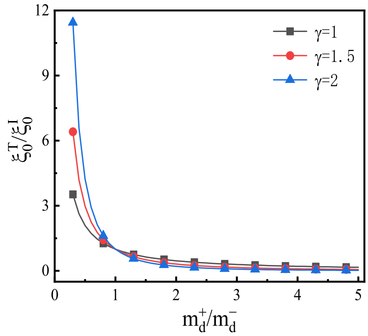

FIGURE 2. Dependence of the amplitude ratio $\xi_0^T/r\xi_0^I$ of transmitted wave to the incident wave on the mass ratio m_d^+/m_d^-, where the parameter $\gamma = 1$, 1.5, 2.

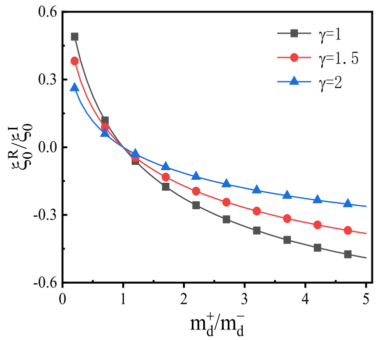

FIGURE 3. Dependence of the amplitude ratio ξ_0^R/ξ_0^I of reflected wave to the incident wave on the mass ratio m_d^+/m_d^-, where the parameter $\gamma = 1$, 1.5, 2.

It is found from figure 3 that there are no reflected waves if the mass of both regions is same. However, there are reflected waves if the dust particle mass in both regions is different. The reflected wave amplitude increases as the mass ratio between the two regions increases. Furthermore, the amplitude ratio of the reflected wave to the incident wave decreases as the parameter γ increases in the region $m_d^+/m_d^- < 1$, while it increases as the parameter γ increases in the region $m_d^+/m_d^- > 1$. There is a phase shift of π for the reflected wave in the region $m_d^+/m_d^- > 1$, while there are no phase shifts in the region $m_d^+/m_d^- < 1$.

Notice that there is no reflection in an homogeneous dust lattice chain, while there is reflection in an inhomogeneous one. This result can be used to determine whether the dust lattice is homogeneous or not.

4.2. *Approximate nonlinear wave equations for incident, transmitted and reflected waves*

In this section, we study the transmission and reflection of a nonlinear wave by using the traditional reductive perturbation method under the condition that the waves satisfy both the small amplitude approximation and the long

Downloaded from https://www.cambridge.org/core. IP address: 18.189.178.124, on 06 Apr 2025 at 16:28:04, subject to the Cambridge Core terms of use, available at https://www.cambridge.org/core/terms. https://doi.org/10.1017/S0022377825000236

wavelength approximation (Su & Mirie 1980; Jeffrey & Kawahara 1982; Ghosh *et al.* 2002; Zhang *et al.* 2014; Gao *et al.* 2017). We introduce the stretched coordinates $\eta^+ = \varepsilon(x - c^+ t)$, $\tau = \varepsilon^3 x$ and $\xi^+ = \varepsilon\xi_1^+ + \varepsilon^3\xi_2^+ + \cdots$ in the region $x > 0$. However, we introduce $\eta^- = \varepsilon(x - c^- t)$, $\zeta^- = \varepsilon(x + c^- t)$, $\tau = \varepsilon^3 x$ and $\xi^- = \varepsilon\xi_1^- + \varepsilon^3\xi_2^- + \cdots$ in the region $x < 0$, where ξ^+ and ξ^- represent physical quantities in the regions $x > 0$ and $x < 0$, respectively, ε is a small parameter, c^+ is the wave speed in the region $x > 0$, and c^- is the wave speed in the region $x < 0$. By substituting these expansions into (2.1), we obtain $c^+ = \sqrt{B_1^+}$, $c^- = \sqrt{B_1^-}$, $\xi_1^+(\eta^+, \tau) = \xi^T(\eta^+, \tau)$, $\xi_1^-(\eta^-, \zeta^-, \tau) = \xi^I(\eta^-, \tau) + \xi^R(\zeta^-, \tau)$, resulting in three Korteweg–de Vries (KdV) equations: $(\partial w^I/\partial\tau) + \alpha^- w^I(\partial w^I/\partial\eta^-) + \beta^-(\partial^3 w^I/\partial\eta^{-3}) = 0$, $(\partial w^T/\partial\tau) + \alpha^+ w^T(\partial w^T/\partial\eta^+) + \beta^+(\partial^3 w^T/\partial\eta^{+3}) = 0$, $(\partial w^R/\partial\tau) + \alpha^- w^R(\partial w^R/\partial\zeta^-) + \beta^-(\partial^3 w^R/\partial\zeta^{-3}) = 0$, where $w^I = \partial\xi^I/\partial\eta^-$, $w^T = \partial\xi^T/\partial\eta^+$, $w^R = \partial\xi^R/\partial\zeta^-$, $\alpha^+ = B_2^+/2B_1^+$, $\alpha^- = B_2^-/2B_1^-$, $\beta^+ = a_0^{+2}/24$ and $\beta^- = a_0^{-2}/24$. One of the solitary wave solutions of the KdV equation can be written as $w^Z = w_m^Z sech^2(\eta^\pm - u_0\tau/D^Z)$, where η^+ and η^- correspond to the regions $x > 0$ and $x < 0$, respectively. Here, Z represents I, R and T for the incident, reflected and transmitted solitary waves, respectively. The parameters are defined as follows: $w_m^Z = 3u_0/\alpha^\pm$ (the wave amplitude), $D^Z = 2\sqrt{\beta^\pm/u_0}$ (the wave width) and u_0 (propagation velocity in the moving coordinate system).

One solitary wave solution in the experimental coordinate system can be rewritten as $\xi^Z = \xi_m^Z \tanh(x - v_g^Z t + x_0^Z/D^Z)$, $u^Z = u_m^Z \mathrm{sech}^2(x - v_g^Z t + x_0^Z/D^Z)$, where $\xi_m^Z = a_0^\pm B_1^\pm\sqrt{6(\varepsilon^2 u_0)^Z}/B_2^\pm$ is the displacement amplitude of the dust particle, $u_m^Z = -6(\varepsilon^2 u_0)^Z B_1^{\pm\frac{3}{2}}/rB_2^\pm$ is the dust particle velocity amplitude, $v_g^Z = \sqrt{B_1^\pm}/1 - (\varepsilon^2 u_0)^Z$ is the wave speed, $D^Z = a_0^\pm/\sqrt{6(\varepsilon^2 u_0)^Z}[1 - (\varepsilon^2 u_0)^Z]$ is the wave width, and x_0^Z is the initial phase of the wave for the incident, reflected and transmitted solitary waves.

4.3. *Scattering method for a KdV solitary wave*

To understand the generation of both transmitted and reflected solitary nonlinear waves at $x = 0$, we use the inverse scattering method (Hong *et al.* 2021). For the KdV equation: $\partial\phi/\partial T - 6\phi(\partial\phi/\partial X) + (\partial^3\phi/\partial X^3) = 0$, with its initial condition $\phi(X, 0) = -(2A/rB^2)sech^2(X/B)$. The number N of generated solitary waves is given by the maximum integer satisfies $\sqrt{A + (1/4)} + (1/2) - N > 0$. The amplitudes A_j of the jth solitary wave is given by $A_j = 2([\sqrt{(}A + 1/4) + (1/2) - j]^2)/B^2$, where $j = 1, 2, \cdots, N$.

Suppose there is an incident solitary wave propagating in the positive x direction in the region $x < 0$, which satisfies the KdV equation of $(\partial w^I/\partial\tau) + \alpha^- w^I(\partial w^I/\partial\eta^-) + \beta^-(\partial^3 w^I/\partial\eta^{-3}) = 0$, where one solitary wave solution is $w^I = w_m^I sech^2(\eta^- - u_0\tau/D^I)$, with $w_m^I = 3u_0/\alpha^-$ and $D^I = 2\sqrt{\beta^-/u_0}$. By substituting $W^I = -6(\beta^-/\alpha^- w^I)$ and $T = \beta^-\tau$, we obtain $(\partial W^I/\partial T) - 6W^I(\partial W^I/\partial\eta^-) + (\partial^3 W^I/\partial\eta^{-3}) = 0$. The solitary wave solution can be rewritten as $W^I = W_m^I sech^2(\eta^- - (\frac{u_0}{\beta^-})T)/d^I$. The initial condition for the incident solitary wave is

Downloaded from https://www.cambridge.org/core. IP address: 18.189.178.124, on 06 Apr 2025 at 16:28:04, subject to the Cambridge Core terms of use, available at https://www.cambridge.org/core/terms. https://doi.org/10.1017/S0022377825000236

$$\frac{\partial W^I}{\partial T} - 6W^I \frac{\partial W^I}{\partial \eta^-} + \frac{\partial^3 W^I}{\partial \eta^{-3}} = 0,$$
$$W^I\,|_{x=0} = W_m^I \mathrm{sech}^2 \frac{\eta^-}{d^I}, \tag{4.13}$$

where $W_m^I = -U_0/2$, $d^I = 2/r\sqrt{U_0}$ and U_0 is an arbitrary parameter controlling the amplitude of the solitary wave.

5. Nonlinear transmitted wave and the nonlinear reflected wave due to an incident solitary wave

5.1. *Construction of the 'initial conditions' for both transmitted nonlinear wave and the reflected nonlinear wave from an incident KdV solitary wave*

We now attempt to find the transmitted and reflected waves resulting from an incident solitary wave at an interface. We can derive the following equations from (4.1) and (4.2):

$$\frac{m_d^- c^-}{a_0^{-3}} \frac{\partial \xi^I}{\partial \eta^-}\,|_{x=0} - \frac{m_d^- c^-}{a_0^{-3}} \frac{\partial \xi^R}{\partial \zeta^-}\,|_{x=0} = \frac{m_d^+ c^+}{a_0^{+3}} \frac{\partial \xi^T}{\partial \eta^+}\,|_{x=0}, \tag{5.1}$$

$$k_1^- a_0^- \frac{\partial \xi^I}{\partial \eta^-}\,|_{x=0} + k_1^- a_0^- \frac{\partial \xi^R}{\partial \zeta^-}\,|_{x=0} = k_1^+ a_0^+ \frac{\partial \xi^T}{\partial \eta^+}\,|_{x=0}\,. \tag{5.2}$$

We have from (5.1) and (5.2),

$$w^T\,|_{x=0} = \frac{2}{\chi_2 + \chi_1} w^I\,|_{x=0}, \tag{5.3}$$

$$w^R\,|_{x=0} = \frac{\chi_2 - \chi_1}{\chi_2 + \chi_1} w^I\,|_{x=0}, \tag{5.4}$$

where $\chi_1 = \sqrt{\frac{m_d^+ (a_0^-)^7}{m_d^- (a_0^+)^7} \frac{q^+}{q^-}}$ and $\chi_2 = (q^+ a_0^- / q^- a_0^+)^2$.

The 'initial conditions' for the transmitted nonlinear wave can be described by the following equations:

$$\frac{\partial W^T}{\partial T} - 6W^T \frac{\partial W^T}{\partial \eta^+} + \frac{\partial^3 W^T}{\partial \eta^{+3}} = 0,$$
$$W^T\,|_{x=0} = \frac{2}{\chi_2 + \chi_1} W_m^I \mathrm{sech}^2 \frac{-\epsilon c^- t}{d^I}, \tag{5.5}$$

where $W^T = -6(\beta^+/\alpha^+) w^T$ and $T = \beta^+ \tau$.

Letting $B^T = c^+ d^I / r c^-$, we have

$$\frac{\partial W^T}{\partial T} - 6W^T \frac{\partial W^T}{\partial \eta^+} + \frac{\partial^3 W^T}{\partial \eta^{+3}} = 0,$$
$$W^T\,|_{x=0} = -\frac{2A^T}{(B^T)^2} \mathrm{sech}^2 [\frac{\eta^+}{B^T}], \tag{5.6}$$

where $A^T = (2/\chi_1 + \chi_2)(m_d^- / m_d^+)((a_0^+ / a_0^-)^2 (k_1^+ / k_1^-)$. In the limit case where $a_0 << \lambda_D$, we have $A^T = (2/\chi_1 + \chi_2)(m_d^- / m_d^+)(a_0^- / a_0^+)(q^+ / q^{-2})$.

Downloaded from https://www.cambridge.org/core. IP address: 18.189.178.124, on 06 Apr 2025 at 16:28:04, subject to the Cambridge Core terms of use, available at https://www.cambridge.org/core/terms. https://doi.org/10.1017/S0022377825000236

Similarly, the 'initial conditions' for the reflected wave can be described by the following equations:

$$\frac{\partial W^R}{\partial R} - 6W^R \frac{\partial W^R}{\partial \zeta^+} + \frac{\partial^3 W^R}{\partial \zeta^{+3}} = 0,$$
$$W^R |_{x=0} = -\frac{2A^R}{(B^R)^2} \mathrm{sech}^2[\frac{\eta^+}{B^R}], \tag{5.7}$$

where $A^R = 2(\chi_2 - \chi_1/\chi_1 + \chi_2)$ and $B^R = d^I$.

5.2. *Transmitted wave and the reflected wave by an interface*

The transmitted nonlinear waves from an indent solitary wave due to the interface can be obtained using (5.6) and the scattering method. The number N^T of generated transmitted solitary waves is given by the maximum integer satisfying the inequality $\sqrt{A^T + (1/4)} + (1/2) - N^T > 0$, where $A^T = (2/\chi_1 + \chi_2)(m_d^-/m_d^+)(a_0^-/a_0^+)((q_d^+/q_d^-)^2)$. In the limit case where $a_0 << \lambda_D$, we have $a_0^+/a_0^- = ((m_d^+/m_d^-))^{-\frac{\gamma}{6}}$, $q^+/q^- = ((m_d^+/m_d^-))^{\frac{\gamma}{3}}$, $\chi_1 = \sqrt{\frac{m_d^+(a_0^-)^7}{m_d^-(a_0^+)^7}}(q^+/q^-) = (m_d^+/m_d^-)^{\frac{1}{2}+\frac{11}{12}\gamma}$, $\chi_2 = ((q^+a_0^-/q^-a_0^+)^2) = ((m_d^+/m_d^-))^{\gamma}$. Then, $A^T = (2/\chi_1 + \chi_2)(m_d^-/m_d^+)^{\frac{5\gamma}{6}-1}$. The corresponding amplitudes of jth transmitted solitary wave, A_j^T, is given by $A_j^T = 2\frac{\sqrt{A^T+(1/4)}+(1/2)-j}{(B^T)^2}$.

The dependence of the number of transmitted solitary waves on the mass ratio (m_d^+/m_d^-) is shown in figure 4, with $\gamma = 1, 1.5, 2$. It shows that there are two transmitted solitary waves when $0.2 < (m_d^+/m_d^-) < 0.6$. For $\gamma = 1.0$, there is only one transmitted solitary wave when $(m_d^+/m_d^-) > 0.6$. However, if $\gamma = 1.5$, the region where two transmitted solitary waves exist is $0.4 < (m_d^+/m_d^-) < 0.6$ and the region for only one transmitted solitary wave is $(m_d^+/m_d^-) > 0.6$. For a larger value of $\gamma = 2$, the region for two transmitted solitary waves is $0.6 < (m_d^+/m_d^-) < 0.8$, while the region for only one transmitted solitary wave is $(m_d^+/m_d^-) > 0.8$. Moreover, the dependence of the amplitude ratio of the transmitted solitary wave to the incident solitary wave on the mass ratio (m_d^+/m_d^-) is shown in figure 5. It seems that the amplitude ratio of the transmitted solitary wave to the incident solitary wave decreases as the mass ration (m_d^+/m_d^-) increases.

Similarly, the reflected nonlinear waves from an indent solitary wave due to the interface are obtained from (5.7) and the scattering method. The number N^R of generated reflected solitary waves is given by the maximum integer of the inequality $\sqrt{A^R + (1/4)} + (1/2) - N^R > 0$, where $A^R = 2(\chi_2 - \chi_1/\chi_1 + \chi_2)$. The corresponding amplitudes of the jth reflected solitary wave A_j^R are given by $A_j^R = 2(\sqrt{A^R + (1/4)} + (1/2) - j(B^R)^2)$.

The dependence of the number of reflected solitary waves on the mass ratio, (m_d^+/m_d^-), is shown in figure 6, where $\gamma = 1, 1.5, 2$. It shows that there is either one reflected solitary wave or none. When $0.2 < (m_d^+/m_d^-) < 1.1$, there is only one reflected solitary wave, while there are no reflected solitary waves when $1.1 < (m_d^+/m_d^-)$. It seems that whether there is one or no reflected solitary waves is independent of the parameter γ.

Downloaded from https://www.cambridge.org/core. IP address: 18.189.178.124, on 06 Apr 2025 at 16:28:04, subject to the Cambridge Core terms of use, available at https://www.cambridge.org/core/terms. https://doi.org/10.1017/S0022377825000236

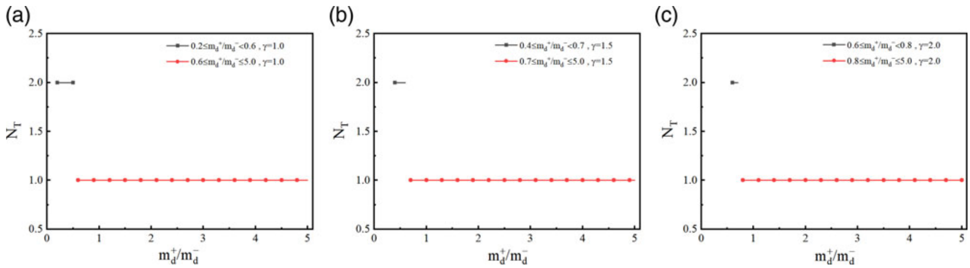

FIGURE 4. Dependence of the number of transmitted solitary waves on the mass ratio m_d^+/m_d^-, with the parameter γ set to (*a*) 1, (*b*) 1.5 and (*c*) 2.

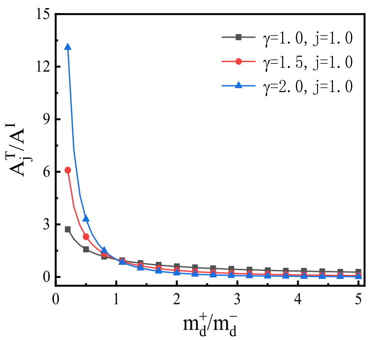

FIGURE 5. Dependence of the amplitude ratio, A_1^T/A^I of the transmitted solitary wave to the incident solitary wave on the mass ratio m_d^+/m_d^-, with the parameter γ set to 1, 1.5 and 2.

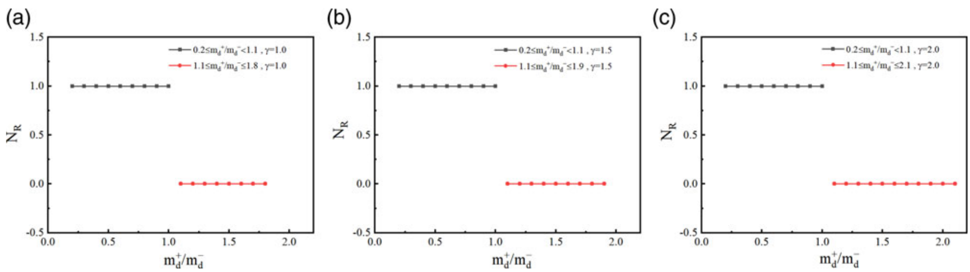

FIGURE 6. Dependence of the numbers of the reflected solitary waves on the mass ratio, m_d^+/m_d^-, where the parameter γ is set to (*a*) 1, (*b*) 1.5 and (*c*) 2.

Moreover, the dependence of the amplitude ratio of the reflected solitary wave to the incident solitary wave on the mass ratio of (m_d^+/m_d^-) is shown in figure 7. It seems that there is no reflection if $m_d^+ = m_d^-$. The amplitude ratio of the reflected solitary wave to the incident solitary wave decreases as the mass ratio (m_d^+/m_d^-) increases in the region $0 < (m_d^+/m_d^-) < 1$, while the amplitude ratio of the reflected solitary wave to the incident solitary wave increases as the mass ratio (m_d^+/m_d^-) increases in the region $(m_d^+/m_d^-) > 1$.

Downloaded from https://www.cambridge.org/core. IP address: 18.189.178.124, on 06 Apr 2025 at 16:28:04, subject to the Cambridge Core terms of use, available at https://www.cambridge.org/core/terms. https://doi.org/10.1017/S0022377825000236

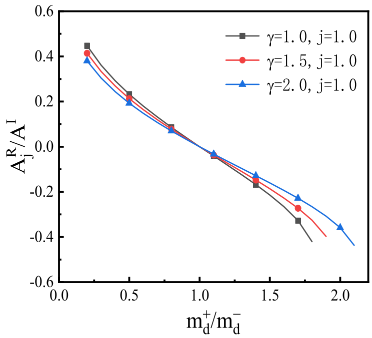

FIGURE 7. Dependence of the amplitude ratio, A_1^R/A^I, of the reflected solitary wave to the incident solitary wave on the mass ratio (m_d^+/m_d^-), with the parameter γ set to 1, 1.5 and 2.

6. Conclusions

As is well known, a dusty plasma typically consists of different species of dust particles, both in space plasma and experimental settings on Earth. However, most investigations on dust acoustic wave in dusty plasma assume that all dust particles are the same. The present paper studies dust acoustic wave propagation in an inhomogeneous dusty plasma and seeks to determine how the inhomogeneity of the dusty plasma affects the dust acoustic wave.

It is found in the present paper that the transmitted wave amplitude decreases for a given incident wave if the incident wave propagates from the smaller dust particle mass region to the larger dust particle mass region, while the transmitted wave amplitude increases if the incident wave propagates from the larger dust particle mass region to the smaller dust particle mass region. It is also found that there is no reflected wave if the dust particle mass of both regions is the same. However, there is a reflected wave if the dust particle mass in both regions is different. The reflected wave amplitude increases as the mass ratio between the two regions increases.

It appears that dust acoustic waves cannot propagate in the dust lattice if the wavelength is sufficiently small. The critical wavelength is $\lambda_c = (\pi/\sqrt{3})a_0$. If $\lambda > \lambda_c$, the wave exists, but it cannot exist if $\lambda < \lambda_c$. This indicates that dust acoustic waves cannot propagate in the dust lattice when the wavelength is smaller than the dust lattice constant.

Using the scattering method and the reductive perturbation method, we find that at least one transmitted solitary wave is generated when an incident solitary wave reaches a discontinuous interface. The number of solitary waves and their corresponding amplitudes depend on the mass ratio between the two regions. However, there can be at most one reflected solitary wave. No reflected solitary wave occurs if an incident solitary wave propagates from a region with smaller dust particle mass into a region with larger dust particle mass.

The present results demonstrate that the mass ratio between two distinct regions in an inhomogeneous dusty plasma plays a crucial role in dust acoustic wave propagation. Based on these findings, we can design an experiment to estimate the mass of the dust particles and identify the locations of different dust species by introducing an incident wave, and analysing both the transmitted and reflected waves. For more complex inhomogeneous dusty plasmas, understanding how transmission and

Downloaded from https://www.cambridge.org/core. IP address: 18.189.178.124, on 06 Apr 2025 at 16:28:04, subject to the Cambridge Core terms of use, available at https://www.cambridge.org/core/terms. https://doi.org/10.1017/S0022377825000236

reflection depend on both the incident wave and the plasma inhomogeneity remains a topic for future research.

Funding

This work was supported by the Gansu Natural Science Foundation (No. 24JRRP004), the novation Fund for University Teachers in Gansu Province (No. 2025A-212) and the Presidents Research Fund High-Level Talent Recruitment Project (Nos. 2023ZCC-02, 2023PY-18).

Declaration of interest

The authors declare that they have no known competing financial interests or personal relationships that could have appeared to influence the work reported in this paper.

REFERENCES

BARKAN, A., D'ANGELO, N. & MERLINO, R.L. 1996 Potential relaxation instability and ion acoustic waves in a dusty plasma. *Planet. Space Sci.* **44** (3), 239–242.

BARKAN, A., MERLINO, R.L. & D'ANGELO, N. 1995 Laboratory observation of the dust-acoustic wave mode. *Phys. Plasmas* **2** (10), 3563–3565.

CHOW, V.W., MENDIS, D.A. & ROSENBERG, M. 1993 Role of grain size and particle velocity distribution in secondary electron emission in space plasmas. *J. Geophys. Res.* **98** (A11), 19065–19076.

DU, C.R., NOSENKO, V., THOMAS, H.M., LIN, Y.F., MORFILL, G.E. & IVLEV, A.V. 2019 Slow dynamics in a quasi-two-dimensional binary complex plasma. *Phys. Rev. Lett.* **123** (18), 185002.

DU, C.R. et al. 2012 Experimental investigation on lane formation in complex plasmas under microgravity conditions. *New J. Phys.* **14** (7), 073058.

DUAN, W.S. 2001 Weakly two-dimensional dust acoustic waves. *Phys. Plasmas* **8** (8), 3583–3586.

DUAN, W.S. & PARKES, J. 2003 Dust size distribution for dust acoustic waves in a magnetized dusty plasma. *Phys. Rev. E* **68** (6), 067402.

DUAN, W.S. & SHI, Y.R. 2003 The effect of dust size distribution for two ion temperature dusty plasmas. *Chaos, Solitons Fractals* **18** (2), 321–328.

DUAN, W.S., YANG, H.J., SHI, Y.R. & LÜ, K.P. 2007 The effects of Gaussian size distribution dust particles in a complex plasma. *Phys. Lett. A* **361** (4-5), 368–372.

FENG, Y., GOREE, J. & LIU, B. 2010 Viscoelasticity of 2D liquids quantified in a dusty plasma experiment. *Phys. Rev. Lett.* **105** (2), 025002.

FENG, Y., LIN, W., LI, W. & WANG, Q.L. 2016 Equations of state and diagrams of two-dimensional liquid dusty plasmas. *Phys. Plasmas* **23** (9), 093705.

GAO, D.N., ZHANG, H., ZHANG, J., LI, Z.Z. & DUAN, W.S. 2017 Effect of a damping force on dust acoustic waves simulated by particle - in - cell method. *Phys. Plasmas* **24** (4), 043703.

GHOSH, S., CHAUDHURI, T.K., SARKAR, S., KHAN, M. & GUPTA, M.R. 2002 Collisionless damping of nonlinear dust ion acoustic wave due to dust charge fluctuation. *Phys. Rev. E* **65** (3), 037401.

GHOSH, S., GUPTA, M.R., CHAKRABARTI, N. & CHAUDHURI, M. 2011 Nonlinear wave propagation in a strongly coupled collisional dusty plasma. *Phys. Rev. E* **83** (6), 066406.

HARTMANN, P., DONK, Z.A, KALMAN, G.J., KYRKOS, S., GOLDEN, K.I. & ROSENBERG, M. 2009 Collective dynamics of complex plasma bilayers. *Phys. Rev. Lett.* **103** (24), 245002.

HE, G.L., ZHAN, Y.F., ZHANG, J.Z. & GE, N. 2016 Characterization of the dynamic effects of the reentry plasma sheath on electromagnetic wave propagation. *IEEE Trans. Plasma Sci.* **44** (3), 232–238.

HEINRICH, J., KIM, S.-H. & MERLINO, R.L. 2009 Laboratory observations of self-excited dust acoustic shocks. *Phys. Rev. Lett.* **103** (11), 115002.

HOMANN, A., MELZER, A., PETERS, S. & PIEL, A. 1997 Determination of the dust screening length by laser-excited lattice waves. *Phys. Rev. E* **56** (6), 7138–7141.

Downloaded from https://www.cambridge.org/core. IP address: 18.189.178.124, on 06 Apr 2025 at 16:28:04, subject to the Cambridge Core terms of use, available at https://www.cambridge.org/core/terms. https://doi.org/10.1017/S0022377825000236

HONG, X.R., SUN, W., SCHWABE, M., DU, C.R. & DUAN, W.S. 2021 Reflection and transmission of an incident solitary wave at an interface of a binary complex plasma in a microgravity condition. *Phys. Rev. E* **104** (2), 025206.

HORANYI, M. & GOERTZ, C.K. 1990 Coagulation of dust particles in a plasma. *Astrophys. J.* **361**, 155.

HOUWE, A., ABBAGARI, S., INC, M., BETCHEWE, G., DOKA, S.Y. & CRÉPIN, K.T. 2022 Envelope solitons of the nonlinear discrete vertical dust grain oscillation in dusty plasma crystals. *Chaos, Solitons Fractals* **155**, 111640.

I, L., JUAN, W.-T., CHIANG, C.-H. & CHU, J.H. 1996 Microscopic particle motions in strongly coupled dusty plasmas. *Science* **272** (5268), 1626–1628.

IVLEV, A.V., ZHDANOV, S.K., THOMAS, H.M. & MORFILL, G.E. 2009 Fluid phase separation in binary complex plasmas. *Europhys. Lett.* **85** (4), 45001.

JEFFREY, A. & KAWAHARA, T. 1982 Asymptotic methods in nonlinear wave theory. *Appl. Math. Ser*. **128**, 223–224.

JIANG, K., HOU, L.J., IVLEV, A.V., LI, Y.F., DU, C.R., THOMAS, H.M., MORFILL, G.E. & SÜTTERLIN, K.R. 2011 Initial stages in phase separation of binary complex plasmas: numerical experiments. *Europhys. Lett.* **93** (5), 55001.

KALMAN, G.J., HARTMANN, P., DONKÓ, Z. & ROSENBERG, M. 2004 Two-dimensional Yukawa liquids: correlation and dynamics. *Phys. Rev. Lett.* **92** (6), 065001.

KILLER, C., BOCKWOLDT, T., SCHÜTT, S., HIMPEL, M., MELZER, A. & PIEL, A. 2016 Phase separation of binary charged particle systems with small size disparities using a dusty plasma. *Phys. Rev. Lett.* **116** (11), 115002.

KOUKOULOYANNIS, V. & KOURAKIS, I. 2009 Single-site and multisite discrete breathers in hexagonal dusty plasma lattices. *Phys. Rev. E* **80** (2), 026402.

KUMAR, K., BANDYOPADHYAY, P., SINGH, S., ARORA, G. & SEN, A. 2021 Reflection of a dust acoustic solitary wave in a dusty plasma. *Phys. Plasmas* **28** (10), 103701.

LI, Z.Z. & DUAN, W.S. 2021 Weak dust acoustic shock wave in strongly coupled two-dimensional complex plasma. *Phys. Plasmas* **28** (4), 043704.

LIN, W., MURILLO, M.S. & FENG, Y. 2019 Pressure and energy of compressional shocks in two-dimensional Yukawa systems. *Phys. Rev. E* **100** (4), 043203.

LIU, B., AVINASH, K. & GOREE, J. 2003 Transverse optical mode in a one-dimensional Yukawa chain. *Phys. Rev. Lett.* **91** (25), 255003.

MARCIANTE, M. & MURILLO, M.S. 2017 Thermodynamic and kinetic properties of shocks in two-dimensional Yukawa systems. *Phys. Rev. Lett.* **118** (2), 025001.

MELZER, A., NUNOMURA, S., SAMSONOV, D., MA, Z.W. & GOREE, J. 2000 Laser-excited mach cones in a dusty plasma crystal. *Phys. Rev. E* **62** (3), 4162–4176.

MELZER, A., SCHELLA, A., SCHABLINSKI, J., BLOCK, D. & PIEL, A. 2013 Analyzing the liquid state of two-dimensional dust clusters: the instantaneous normal mode approach. *Phys. Rev. E* **87** (3), 033107.

MENDIS, D.A. & ROSENBERG, M. 1994 Cosmic dusty plasma. *Annu. Rev. Astron. Astrophys.* **32** (1), 419–463.

MEURIS, P., VERHEEST, F. & LAKHINA, G.S. 1997 Influence of dust mass distributions on generalized Jeans–Buneman instabilities in dusty plasmas. *Planet. Space Sci.* **45** (4), 449–454.

MORFILL, G.E. & IVLEV, A.V. 2009 Complex plasmas: an interdisciplinary research field. *Rev. Mod. Phys.* **81** (4), 1353–1404.

MURILLO, M.S. 2000 Critical wave vectors for transverse modes in strongly coupled dusty plasmas. *Phys. Rev. Lett.* **85** (12), 2514–2517.

NOSENKO, V., GOREE, J. & PIEL, A. 2006 Cutoff wave number for shear waves in a two-dimensional Yukawa system (dusty plasma). *Phys. Rev. Lett.* **97** (11), 115001.

NUNOMURA, S., GOREE, J., HU, S., WANG, X. & BHATTACHARJEE, A. 2002 Dispersion relations of longitudinal and transverse waves in two-dimensional screened Coulomb crystals. *Phys. Rev. E* **65** (6), 066402.

OXTOBY, N.P., GRIFFITH, E.J., DURNIAK, C., RALPH, J.F. & SAMSONOV, D. 2013 Ideal gas behavior of a strongly coupled complex (dusty) plasma. *Phys. Rev. Lett.* **111** (1), 015002.

Downloaded from https://www.cambridge.org/core. IP address: 18.189.178.124, on 06 Apr 2025 at 16:28:04, subject to the Cambridge Core terms of use, available at https://www.cambridge.org/core/terms. https://doi.org/10.1017/S0022377825000236

RAO, N.N., SHUKLA, P.K. & YU, M.Y. 1990 Dust-acoustic waves in dusty plasmas. *Planet. Space Sci.* **38** (4), 543–546.

SERGEEV, E.N. & GRACH, S.M. 2014 Study of the plasma turbulence dynamics by measurements of diagnostic stimulated electromagnetic emission. i. experimental results. *Radiophys. Quant. Electron* **57** (2), 81–99.

SHUKLA, P.K. & ELIASSON, B. 2012 Nonlinear dynamics of large-amplitude dust acoustic shocks and solitary pulses in dusty plasmas. *Phys. Rev. E* **86** (4), 046402.

SMITH, B., HYDE, T., MATTHEWS, L., REAY, J., COOK, M. & SCHMOKE, J. 2008 Phase transitions in a dusty plasma with two distinct particle sizes. *Adv. Space Res.* **41** (9), 1510–1513.

SU, C.H. & MIRIE, R.M. 1980 On head-on collisions between solitary waves. *J. Fluid Mech.* **98** (03), 509.

SUN, W. *et al.*et al. 2018 Dissipative solitary wave at the interface of a binary complex plasma. *Europhys. Lett.* **122** (5), 55001.

THOMAS, H., MORFILL, G.E., DEMMEL, V., GOREE, J., FEUERBACHER, B. & MÖHLMANN, D. 1994 Plasma crystal: Coulomb crystallization in a dusty plasma. *Phys. Rev. Lett.* **73** (5), 652–655.

THOMAS, E., KONOPKA, J., MERLINO, U., R., L. & ROSENBERG, M. 2016 Initial measurements of two- and three-dimensional ordering, waves, and plasma filamentation in the magnetized dusty plasma experiment. *Phys. Plasmas* **23** (5), 055701.

WEI, L., PENG, Y., YANG, Y.Y., WANG, F.P., YANG, L. & DUAN, W.S. 2023 Transmission and reflection of an incident pulse in a chain of dust particles. *Results Phys.* **52**, 106779.

WIEBEN, F., SCHABLINSKI, J. & BLOCK, D. 2017 Generation of two-dimensional binary mixtures in complex plasmas. *Phys. Plasmas* **24** (3), 033707.

XU, G.J. & SONG, Z.H. 2019 Interaction of terahertz waves propagation in a homogeneous, magnetized, and collisional plasma slab. *Waves Random Complex Media* **29** (4), 665–677.

YANG, L., SCHWABE, M., ZHDANOV, S., THOMAS, H.M., LIPAEV, A.M., MOLOTKOV, V.I., FORTOV, V.E., ZHANG, J. & DU, C.R. 2017 Density waves at the interface of a binary complex plasma. *Europhys. Lett.* **117** (2), 25001.

ZHANG, J., YANG, Y., XU, Y.X., YANG, L., QI, X. & DUAN, W.S. 2014 The study of the poincare - lighthill - kuo method by using the particle - in - cell simulation method in a dusty plasma. *Phys. Plasmas* **21** (10), 103706.

Downloaded from https://www.cambridge.org/core. IP address: 18.189.178.124, on 06 Apr 2025 at 16:28:04, subject to the Cambridge Core terms of use, available at https://www.cambridge.org/core/terms. https://doi.org/10.1017/S0022377825000236